

## Wave-Vector Dependence of the Jahn-Teller Interactions in $\text{TmVO}_4$

J. K. Kjems

*Danish Atomic Energy Research Establishment Risø, DK-4000 Roskilde, Denmark*

and

W. Hayes and S. H. Smith

*Clarendon Laboratory, Oxford, United Kingdom*

(Received 25 August 1975)

The resonant Jahn-Teller coupling of the  $B_{2g}$  acoustic phonon and the Zeeman-split ground doublet in  $\text{TmVO}_4$  has been studied by inelastic neutron scattering. Tuning of the magnetic field provides a means for investigating the wave-vector dependence of the interactions. We find that the coupling is constant in the region where the phonon dispersion is linear, up to 0.4 of the distance to the zone boundary. This agrees with the predictions of a Debye model.

Interest in the cooperative Jahn-Teller effect has increased considerably in recent years.<sup>1</sup> In particular, studies of the rare-earth (RE) insulators have revealed a gratifying accord between the simple mean-field and random-phase-approximation (RPA) theories devised by Elliott *et al.*<sup>2</sup> and the bulk of the experimental evidence<sup>1</sup> obtained by fluorescence spectroscopy, Raman and Brillouin scattering, ultrasonics, x-ray and neutron diffraction, and inelastic neutron scattering. Among the systems studied so far, one has proven to be exceedingly simple, namely  $\text{TmVO}_4$ . Here we have the classical Jahn-Teller situation with an orbital doublet ground state of the  $\text{Tm}^{+3}$   ${}^3H_6$  multiplet, which is split by a spontaneous lattice distortion from tetragonal ( $D_{4h}^{19}$ ) to orthorhombic symmetry ( $D_{2h}^{24}$ ) at  $T_D = 2.1$  K.<sup>3</sup> The ground doublet is well separated from the first excited state (a singlet at  $60 \text{ cm}^{-1}$  observed in the course of the present work). An optical study<sup>3</sup> of the splitting,  $2\Delta$ , of the doublet below  $T_D$  has shown that at saturation  $\Delta = kT_D$  in accordance with the mean-field expectation. Similarly, the specific-heat anomaly<sup>4</sup> is well reproduced by the theory. A Raman-scattering study<sup>5</sup> has established that the acoustic strain coupling dominates, and detailed measurements of the elastic constants<sup>6</sup> have shown that the important strain has  $B_{2g}$  symmetry. All of the measurements performed so far have probed either zone-center or zone-averaged quantities. Here we report an investigation of the wave-vector dependence of the Jahn-Teller coupling to the  $B_{2g}$  acoustic phonon. The information is obtained by observation of the resonant interaction between the Zeeman-split ground state ( $H$  parallel to the crystallographic  $c$  axis) and the transverse phonon. As the field

is increased the crossing point moves into the zone and this provides a novel method for the direct study of the wave-vector dependence of quadrupole matrix elements.  $\text{TmVO}_4$  lends itself conveniently to such investigations because of the large spectroscopic splitting factor,<sup>5</sup>  $g_{\parallel} = 10.6$ , for the ground doublet. Furthermore, the studies of temperature dependence of the elastic constants<sup>6</sup> have yielded precise quantitative values for the zone-center couplings, and the simple Debye model for electron-phonon interactions predicts that the couplings are independent of the magnitude of the wave vector, but that they have a strong directional dependence as one moves out into the zone. Our results correspond exactly to these predictions and hence they confirm that  $\text{TmVO}_4$  is an ideal model Jahn-Teller system.

The measurements were performed at the Risø DR3 reactor on a cold-source triple-axis spectrometer working in the constant- $Q$  mode. The incident energy was fixed at  $14.26 \text{ meV}$  ( $k_i = 2.623 \text{ \AA}^{-1}$ ). At this energy the cold-source spectrum contains a negligible amount of higher-order contamination. Curved and planar pyrolytic graphite crystals acted as monochromator and analyzer, respectively, using the (002) planes in reflection. The horizontal collimations were typically  $45'$  throughout the spectrometer and the vertical spread was about  $4^\circ$ . The  $\text{TmVO}_4$  sample was pulled from a flux and was a transparent crystal with dimensions  $6 \times 6 \times 10 \text{ mm}^3$  and with mosaic spread less than  $0.2^\circ$ . The sample was mounted in an Oxford Cryogenics 45-kG superconducting magnet with the field axis vertical and parallel to the crystallographic  $c$  axis. The present measurements were confined to the  $B_{2g}$  transverse

acoustic phonon along the  $a^*$  direction whose slope is given by  $(C_{66}/\rho)^{1/2}$  with  $\rho = 6.80 \text{ g/cm}^3$ . They were made at liquid-helium temperatures, i.e., above the spontaneous Jahn-Teller transition at 2.1 K. Figure 1 shows examples of the observed scattering profiles with and without the applied magnetic field. The line shape without field can be accounted for by the known resolution function corresponding to the actual spectrometer configuration. The line shape with the field shows that the resonant interaction of the Zeeman-split doublet and the phonon produces two peaks whose integrated intensities correspond to the zero-field phonon within the experimental error. This is expected since no dipole transitions exist between the completely polarized  $|\pm 5\rangle$  and  $|\pm 1\rangle$  states.<sup>1,3</sup>

The interaction between the electronic quadrupole operators and the local strains,  $\epsilon_{ij}$ , can be treated in a pseudospin formalism<sup>2</sup> with the following Hamiltonian:

$$\mathcal{H} = \sum_{\vec{k}, p} \omega_p(\vec{k}) (a_{\vec{k}}^\dagger + a_{-\vec{k}} + \frac{1}{2}) + \sum_{\vec{k}, n} \exp(i\vec{k} \cdot \vec{R}_n) \xi_{ij}(\vec{k}) S_n^z (a_{\vec{k}}^\dagger + a_{-\vec{k}}^\dagger) + g\mu_B H \sum_n S_n^x, \quad (1)$$

where  $n$  is a site index,  $\omega_p(\vec{k})$  is a phonon frequency at wave vector  $\vec{k}$ , and  $S_n^z$  refers to a quadrupole moment in the plane perpendicular to the crystallographic  $c$  axis (the field axis). The Debye model for local strain due to an acoustic phonon with eigenvector  $\vec{e}(\vec{k})$  gives

$$\xi_{ij}(\vec{k}) = V_s^{-1/2} i [\hbar/2M\hbar\omega_p(\vec{k})]^{1/2} [k_i e_j(\vec{k}) + k_j e_i(\vec{k})]. \quad (2)$$

In the region where  $\omega_p(k) = Ck$  one has  $\xi \propto k^{1/2}$ . A displaced oscillator transformation brings the problem into the form of the Ising model in a transverse field with

$$\gamma_{\vec{k}} = a_{\vec{k}} + \frac{\xi(\vec{k})}{\hbar\omega_p(\vec{k})} S_{\vec{k}}^z, \quad K_p(\vec{k}) = \frac{|\xi(\vec{k})|^2}{\hbar\omega_p(\vec{k})}, \quad 2\Delta = g\mu_B H, \quad (3)$$

so that

$$\mathcal{H} = \sum_{\vec{k}} \hbar\omega_p(\vec{k}) (\gamma_{\vec{k}}^\dagger \gamma_{\vec{k}} + \frac{1}{2}) - \sum_{p, \vec{k}} K_p(\vec{k}) S_{\vec{k}}^z S_{-\vec{k}}^z + \Delta N^{1/2} S_0^x. \quad (4)$$

The mean-field solution for the last two terms only gives the well-known dispersion relation for the so-called quadrupole exciton<sup>7</sup> or vibron<sup>1</sup> for  $T > T_D$ :

$$\hbar^2 \omega_v^2(\vec{k}) = 4\Delta [\Delta - \langle S^x \rangle J(\vec{k})], \quad (5)$$

where

$$J(\vec{k}) = \sum_p K_p(\vec{k}) - N^{-1} \sum_{p, \vec{k}} K_p(\vec{k}) \quad (6)$$

is the effective ion-ion interaction corrected for the self-energy.  $\langle S^x \rangle = \tanh(\Delta/kT)$  for a two-level system. Since  $\gamma_{\vec{k}}$  and  $S_{\vec{k}}^x$  do not commute, Eq. (4) gives rise to mixed phonon-vibron modes

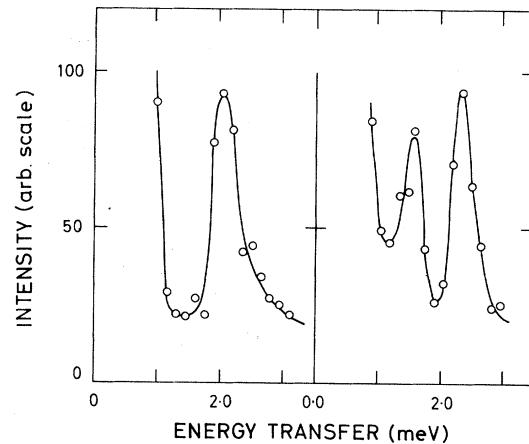


FIG. 1. The observed scattering profiles at 4.5 K for the transverse  $B_{2g}$  acoustic phonon propagating along  $a^*$  and polarized along  $b^*$  at  $q = 0.2$  reciprocal lattice units (rlu) ( $a^* = b^* = 0.8886 \text{ \AA}^{-1}$ ). The left-hand side shows the result in zero external field and the right-hand side shows the effect of an applied field of 26.7 kG. The full lines are drawn as guides to the eye.

which in the RPA are solutions of<sup>1</sup>

$$\hbar\omega(\vec{k}) [\omega^2(\vec{k}) - \omega_v^2(\vec{k})] = \sum_p \frac{4D \langle S^x \rangle \omega^3(\vec{k}) K_p(\vec{k})}{\omega^2(\vec{k}) - \omega_p(\vec{k})}. \quad (7)$$

For coupling to the  $B_{2g}$  acoustic phonon only, the Debye model, Eqs. (2) and (3), predicts that  $K(\vec{k})$  and hence  $J(\vec{k})$  are independent of  $|\vec{k}|$ :

$$K(|\vec{k}|) = \lim_{\vec{k} \rightarrow 0} K(|\vec{k}|) = \mu, \quad J(|\vec{k}|) = \lambda + \mu. \quad (8)$$

These predictions are readily tested by compari-

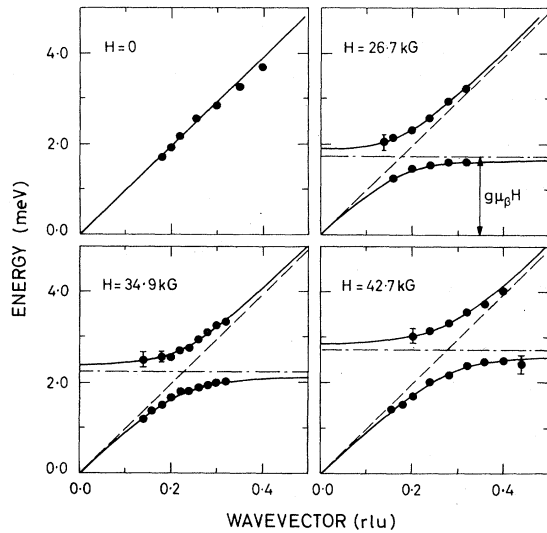


FIG. 2. Mixed-mode dispersion in  $\text{TmVO}_4$  at 4.5 K for external magnetic fields along  $c^*$  with strengths of 0, 26.7, 34.9, and 42.7 kG. The full circles correspond to observed peak positions in the inelastic scans. The full lines correspond to calculations described in the text with the following parameter values:  $g_{\parallel}=10.6$ ,  $C_{66}=1.90 \times 10^{11}$  erg/cm $^2$ ,  $\rho=6.80$  g/cm $^3$ ,  $\lambda=-1.5$  cm $^{-1}$ , and  $\mu=1.8$  cm $^{-1}$ . The broken lines illustrate the unperturbed phonon dispersion and the Zeeman splitting, respectively.

son with the observed anticrossings shown in Fig. 2. To that end we have solved Eq. (7) with  $\mu=1.8$  cm $^{-1}$ ,  $\lambda=-1.5$  cm $^{-1}$ ,  $C_{66}=1.90 \times 10^{11}$  erg/cm $^2$ , and  $g=10.6$  for fields of 0, 26.7, 34.9, and 42.6 kG, respectively. The surface demagnetization field for the oblong sample shape was estimated to  $\pm 1$  kG. The correction due to the dipolar field from sources within the Lorentz sphere has been shown $^8$  to be negligible at finite wave vectors, whereas for static measurements it would reduce the local field by 1.1 kG. $^5$  The resulting dispersion curves are drawn as full lines in Fig. 2.

The accord with the observed excitation frequencies is evident and it constitutes the first confirmation of the Debye picture for the electron-phonon coupling. In a more detailed analysis Eq. (7) has been inverted point by point to give  $K(\vec{k})$  and  $\omega_v(\vec{k})$  directly. We find that both  $K(\vec{k})$  and  $J(\vec{k})$  are independent of magnetic field and of  $|\vec{k}|$  in the examined ranges, within  $\pm 0.1$  cm $^{-1}$ . The parameter values  $C_{66}=(1.90 \pm 0.03) \times 10^{11}$  erg/cm $^2$  and  $\mu=1.8 \pm 0.1$  cm $^{-1}$  are in excellent agreement with values derived at  $k \approx 0$  from the temperature dependence of elastic constants ( $\mu=1.85$  cm $^{-1}$ ,  $\lambda=-0.74$  cm $^{-1}$ , and  $C_{66}^{\infty}=1.933 \times 10^{11}$  cm $^{-1}$ ),

whereas the numerical value for  $\lambda$  is somewhat larger. This is not unexpected since both exchange and dipolar field effects can result in a larger effective  $g$  value at finite wave vector than the one observed by the Raman scattering $^5$  at  $k \approx 0$ . These effects could reduce the  $\lambda$  value by as much as 1 cm $^{-1}$  which would resolve the discrepancy. We have also studied the temperature dependence of the anticrossing at 42.7 kG. The changes are satisfactorily accounted for at temperatures up to 120 K when the temperature dependence of  $\langle S^x \rangle$  is included in Eq. (7).

In conclusion, we stress that  $\text{TmVO}_4$  now has been shown to be an ideal model system for both the static and dynamic properties of the cooperative Jahn-Teller effect. It is remarkable that within the mean-field, RPA, and Debye theories a single set of parameter values describes the details of the field and temperature dependences of such varied quantities as the order parameter, $^3$   $\Delta_0(H, T)$ , the elastic constant, $^6$   $C_{66}(H, T)$ , the susceptibility, $^4$   $\chi(T)$ , the specific heat, $^4$   $C_v(T)$ , and the mixed-mode frequencies,  $\omega(k, H, T)$ , in the field and temperature ranges where the ground doublet can be regarded as isolated. We are currently investigating the effects of fields up to 90 kG. This may reveal directly the coupling to excited states which were inferred from an acoustic anomaly. $^6$  We are also investigating central mode scattering associated with the ground doublet.

The simple result for the wave-vector dependence of the Jahn-Teller couplings in  $\text{TmVO}_4$  is in contrast with the findings for the only other similar mixed-mode system studied so far, namely, the 151-K transition in  $\text{PrAlO}_3$ . $^7$  Here the results show a very strong wave-vector dependence over the same region of the zone. However a strongly dispersed optical phonon mode plays a major role in  $\text{PrAlO}_3$  and this may account for the difference.

The authors wish to acknowledge contributions from discussions with W. J. L. Buyers, P.-A. Lindgård, B. Lüthi, and I. Robinson. One of us (W. H.) is indebted to The Royal Society for support under the European Science Exchange Programme.

$^1$ G. A. Gehring and K. A. Gehring, Rep. Prog. Phys. **38**, 1 (1975).

$^2$ R. J. Elliott, R. T. Harley, W. Hayes, and S. R. P. Smith, Proc. Roy. Soc., Ser. A **328**, 217 (1972).

$^3$ P. J. Becker, M. J. M. Leask, and R. N. Tyte, J.

Phys. C: Solid State Phys. 5, 2027 (1972).

<sup>4</sup>A. H. Cooke, S. J. Swithenby, and M. R. Wells, Solid State Commun. 10, 265 (1972).

<sup>5</sup>R. T. Harley, W. Hayes, and S. R. P. Smith, J. Phys. C: Solid State Phys. 5, 1501 (1972).

<sup>6</sup>R. L. Melcher, E. Pytte, and B. A. Scott, Phys. Rev. Lett. 31, 307 (1973).

<sup>7</sup>R. J. Birgeneau, L. G. van Uitert, J. K. Kjems, and G. Shirane, Phys. Rev. 10, 2512 (1974).

<sup>8</sup>P. -A. Lindgård, private communication.

## Chemisorption Bond Length and Binding Location of Oxygen in a $p(2 \times 1)$ Overlayer on W(110) Using a Convergent, Perturbative, Low-Energy-Electron-Diffraction Calculation\*

M. A. Van Hove and S. Y. Tong

*Department of Physics and Surface Studies Laboratory, University of Wisconsin, Milwaukee, Milwaukee, Wisconsin 53201*

(Received 23 June 1975)

A convergent perturbation scheme known as the layer-doubling method is used to determine the chemisorption position and bond length of an oxygen  $p(2 \times 1)$  overlayer on W(110) surface. The use of perturbation treatment allows accurate and economical determination of surface crystallography on this strong-scattering material. Using eight phase shifts and 89 beams in the calculation, the oxygen atoms are found to occupy threefold-coordinated binding sites with a bond length of 2.08 Å.

The transition metal tungsten is probably the material most used as a substrate for chemisorption of gas atoms and molecules on its different crystal planes. Studies of surface properties of clean tungsten and the chemisorption of various gases on its surfaces have been carried out for many years using different surface-sensitive techniques. However, partly because of the very large atomic weight of the tungsten atom, there has been no accurate surface-structure determination of adsorbed atoms on any of the tungsten surfaces. We report here the first successful determination of surface structure of chemisorbed atoms on a tungsten surface. The binding location and chemisorption bond length of the  $p(2 \times 1)$  oxygen overlayer on W(110) surface are determined using a convergent perturbation calculation<sup>1</sup> of the dynamical low-energy-electron-diffraction (LEED) approach. Our results here also differ from previous surface structures of overlayers determined on other metal substrates<sup>2</sup> in the following way. In all previous studies, the adsorbed foreign atoms settle at those surface sites that an atom of that substrate material would adsorb at, i.e., the bulk structure of the substrate extends into the overlayer. However, in the present case we find evidence to suggest that the oxygen atoms adsorbed on the W(110) surface do not reproduce the bulk structure of the substrate, but rather choose a site of higher coordination number to the substrate (a threefold-coordinated site).

The structures of clean W(100) and W(110) are

first determined.<sup>3</sup> Our results show that for W(100) there is a possible contraction of about 6% of the topmost tungsten layer. On the W(110) surface, we find no contraction, expansion, or lateral shift of the topmost tungsten layer. Details of the surface structures on clean W(100) and W(110) are presented elsewhere.<sup>3</sup> Recently Lagally, Buchholz, and Wang<sup>4</sup> have used the constant-momentum-transfer averaging scheme on W(110) and come to the same conclusion that the (110) surface does not deviate from the bulk structure. In their averaging method, they concentrated on incident electron energies above 150 eV, because below 150 eV the averaging scheme is much more difficult to use. Since our dynamical analyses are primarily done at energies below 200 eV (15 to 200 eV), the agreement between our results and those of Ref. 4 on the surface structure of clean W(110) is significant as it demonstrates the consistency of the two methods using experimental data with almost mutually exclusive energy ranges.

For the  $p(2 \times 1)$  oxygen overlayer on W(110), a number of surface structures have previously been suggested. However, the results of Lagally, Buchholz, and Wang<sup>4</sup> showed that, contrary to previous speculations, there is no reconstruction of the tungsten atoms by the oxygen overlayer. Because they worked at energies above 150 eV, the averaging technique cannot tell the position of the oxygen atom. For a simple  $p(2 \times 1)$  oxygen overlayer on W(110), we show in Fig. 1